International Journal of Engineering

Journal Homepage: www.ije.ir

Performance of a Two-stages Gas Gun: Experimental, Analytical and Numerical Analysis

G. H. Majzoobi*[a], M. H. Ghaed Rahmati[a], M. Kashfi[b]

[a] *Department of Mechanical Engineering, Bu-Ali Sina University, Hamedan, Iran*
[b] *Department of Mechanical Engineering, Ayatollah Boroujerdi University, Boroujerd, Iran*

PAPER INFO

Paper history:
Received 21 July 2018
Received in revised form 03 March 2018
Accepted 19 May 2019

Keywords:
Two Stages Gas Gun
Rajesh Theory
Simulation
Projectile
Autodyn

ABSTRACT

Two stages gas guns are used for various purposes, particularly for mechanical characterization of materials at high rate of deformations. The performance of a two stages gas gun is studied in this work using the theory of the two-stage gas gun proposed by Rajesh, numerical simulation using combined Eulerian/ Lagrangian elements in Autodyna commercial code and experiment using a two stage gas gun developed by the authors of this study. Equations governing the motion of the piston and projectile are solved using Runge-Kutta method. The effects of parameters such as chamber pressure, pump tube pressure and piston mass on the performance of gun are explored. The results of numerical simulation and analytical methods are validated by experiment. Finally, a comparison between the analytical, numerical and experimental results shows that the theory proposed by Rajesh, yields reasonable predictions for the two stage gas gun performance in the first place, and Autodyn software, using combined Eulerian/ Lagrangian elements, gives accurate estimations for gas gun parameters, in the second place. A 3-D working diagram is provided for prediction of projectile velocity for any state of pump and chamber pressures which are the most important variables for a gas gun with a fixed geometry.

***doi**: 10.5829/ije.2019.32.05b.18*

NOMENCLATURE

a_0	Initial sound speed in the chamber light gas	P_{l_0}	Launch tube initial pressure
a_r	Sound speed in the pump tube light gas at the rupture of the second diaphragm	P_r	Pressure at the instant of second diaphragm breakage
d_d	Pump tube diameter	t_p	Time of piston motion
d_l	Launch tube diameter	t_{pr}	Time of projectile motion
l_d	Pump tube length	u_p	Piston speed
l_l	Launch tube length	u_{pr}	Projectile speed
M_e	Mach number	x_p	Piston position inside pump tube
m_p	Piston mass	x_{pr}	Position of projectile inside launch tube
m_{pr}	Projectile mass	**Greek Symbols**	
P_0	Chamber initial pressure	γ_0	Initial gas specific heat ratio
P_b	Shock compression pressure at the projectile base	γ_d	Instant gas specific heat ratios inside pump tube
P_{d_0}	Pump tube initial pressure	λ	The ratio of the initial gas volume in the pump tube and the gas volume at the instant of the second diaphragm breakage
P_d	Instant pump tube pressure ahead of piston		

1. INTRODUCTION

Gas gun is a multipurpose device, which is widely used for launching a projectile. In a conventional single-stage gas gun the high-pressure gas compressed in a chamber is suddenly released to accelerate the projectile inside the launch tube or the barrel of the gun. The gas guns can be categorized as single-stage, two stages and recently three

*Corresponding Author Email: *gh_majzoobi@basu.ac.ir* (G. H. Majzoobi)

Please cite this article as: G. H. Majzoobi, M. H. Ghaed Rahmati, M. Kashfi, Performance of a Two-stages Gas Gun: Experimental, Analytical and Numerical Analysis, International Journal of Engineering (IJE), IJE TRANSACTIONS B: Applications Vol. 32, No. 5, (May 2019) 759-768

stages guns. The gas gun studied in this work is a two-stages one. Two stages gas gun is widely used for mechanical characterization of materials. Taylor [1], flying plate [2], powder compaction [3] and ballistic [4] tests are among the material characterizing and production tests which are accomplished using gas gun. The schematic view of a two-stages gas gun is shown in Figure 1. As the figure shows, a two-stages gas gun consists of a pressure vessel (or chamber), two diaphragms, a piston, a shock (or pump) tube, a conic tube, and a lunch tube. The piston is accelerated by the release of a high-pressure gas compressed in the vessel. The piston movement gives rise to the increase of the pressure of the gas inside the pump tube that may have already been compressed to a desired level of pressure. The piston is trapped by the conic tube and the second diaphragm is burst by the high-pressure gas compressed in the pump tube. The compressed gas ahead of the piston accelerates the projectile inside the launch tube.

If the pressure in the launch tube and behind the projectile remains constant, p, then the muzzle velocity of the projectile is approximated from the following relation:

$$V_0 = \sqrt{2p\frac{AL}{m}} \tag{1}$$

Where A, L and m are the cross sectional area and length of the lunch tube and m is the projectile mass. However, p is not constant and it reduces as the gas expands as follows:

$$P = P_0\left(1-\frac{V}{\left(2/(\gamma-1)\right)a_0}\right)^{2\gamma/(\gamma-1)} \tag{2}$$

In which v is the expansion speed of the gas, γ is the specific heat capacity and a_0 is the sound speed in the gas. If we assume that all the energy of the compressed gas is consumed for the gas mass itself, then it can be shown that the projectile velocity is obtained from the following relation:

$$V_0 = \left(\frac{2}{\gamma-1}\right)a_0 = \left(\frac{2}{\gamma-1}\right)\sqrt{\frac{\gamma RT_0}{M}} \tag{3}$$

As Equation (3) implies, the projectile velocity varies with gas type and gas temperature. Therefore, the highest velocity is obtained for hydrogen and helium. Many investigations have been performed to explore various features of two stages gas guns.

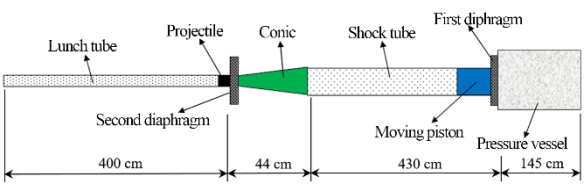

Figure 1. The schematic view of a two-stages gas gun

The concept of two stages gas gun is old [5-10] but its ever increasing application has demanded new development in this area. Moritoh et al. [11] developed a two-stage gas gun and optimized its operating parameters to reach speeds higher than 9 km/s. Lexow et al. [12] made a new two stages gas gun for cratering study. The gun is capable of accelerating projectile masses of up to 100 g to velocities up to 6 km/s. Putzar and Schaefer [13] developed a new two-stage gas gun with two parallel pumps which are attached to a single pressure chamber. Linhart and Cattani [14] argued theoretically that higher efficiency can be achieved for a gas gun if a second diaphragm is used to transfer the kinetic energy of the first piston to the projectile. The limitations of two stages gas guns have been discussed by Glenn [15]. He believes that the velocities up to 10 km/s can be achieved by conventional two stage gas guns. The higher velocities up to 30 km/s are attainable but some limitations in the tests must be admitted.

Francesconi et al. [16, 17] performed a theoretical and numerical investigation to increase the performance of two stage light-gas guns by altering their working conditions. Rajesh et al. [18] presented a mathematical approach to study a flying projectile. The derived differential equations governing the piston and projectile motions were solved using Runge-Kutta methods. They examined the effect of various gas parameters such as piston and projectile mass on the projectile speed. Rajesh et al. [19] also investigated the effect of adding a pump tube in between the pump tube and launch tube and its influence on the efficiency of the gun. Rajesh et al. [20] investigated the fluid dynamic features of the compression process in the pump tube of a ballistic range and to assess how it affects the performance of the ballistic range.

The primary objective of gas gun invention was to perform hypervelocity impacts for military applications. However, today the use of these devices have been extended to other areas and in particular to the area of material characterization or even material fabrications. Doolan [21] proposed a two-stage light gas gun for the investigation of high speed impact in solid rocket propellants. Fredenburg et al. [17] used a three-capsule gas-gun compaction geometry for dynamic compaction of nanocrystalline aluminum alloy powders. Kawai et al. [22] presented a single microparticle launching method to simulate the hypervelocity impacts of micrometeoroids and microdebris on space structures. Schäfer and Janovsky [23] used a sensor network to detect hypervelocity impacts on aircraft structures. They performed their experiment using a gas gun for launching the specimens against the target. Gas guns can be used to obtain the pressure-volume relations known as equation of states which is important at hypervelocity impacts. Jones [24] presented an experimental set up to a driver plate against a target at velocities up to 8 km/s using gas

gun at velocities up to 8 km/s to obtain Hugoniet data from which equation of states are constituted.

In the present study, a two-stages gas gun mainly designed and manufactured for material testing is described. The features of the gas gun in studied by numerical simulations using the Autodyn commercial software. The features are also investigated using the theory of Rajesh [18-20]. The effect of parameters such as the chamber and pump tubes pressures and piston mass on performance of the gun is evaluated. Finally, the numerical predictions and analytical results are validated by experiment. The gas gun presented in this study can be used for Taylor, ballistic and flying impact test. These three tests are highly beneficial for mechanical characterization of materials at high strain rates. It can also be used for some miscellaneous examinations such as dynamic powder compaction. For a two-stages gas gun with fixed geometry, pump and chamber pressures are the most important variables which have significant effect on projectile velocity. The 3-D working diagram for prediction of projectile velocity for any state of pump and chamber pressures the gas gun developed in this work is presented.

2. RAJESH THEORY

Rajesh et al. [18-20] studied analytically the effects of important parameters such as pump tube pressure, piston mass, type of light gas, and the diameters of pump and launch tubes on the performance of two stages gas gun. They used the fifth order Rung-Kutta method to solve the resultant equations ignoring the effect of viscosity and heat transfer. They used isentropic analysis for the expansion and compression of the gases in the chamber and the pump tube, respectively. In their analysis, the equation governing the motion of piston inside the pump tube is obtained as follows:

$$m_p\left(\frac{d^2x_p}{dt_p^2}\right)=\frac{\pi d_d^2}{4}\{p_0[1-\frac{u_p}{a_0}(\frac{\gamma_0-1}{2})]^{2\gamma_0/(\gamma_0-1)} - p_{d_0}\lambda^{-\gamma_d}\} \quad (4)$$

$$x(0)=0 \quad , \quad \dot{x}(0)=0$$

In which d_d is the pump tube diameter, m_p is the piston mass, x_p is the position of the piston inside the pump tube, t_p is the time during piston motion, P_{d0} is pump tube initial pressure and P_0 is the initial chamber pressure. u_p is the piston speed, a_0 is the sound speed in the uncompressed gas in the pump tube. Similar analysis gives the equation governing the projectile speed inside the launch tube as follows:

$$\left(\frac{d^2x_{pr}}{dt_{pr}^2}\right)=\frac{\pi d_l^2 p_r}{4m_{pr}}\{g[1-g^{(1-\gamma_d)/2\gamma_d)} \frac{\gamma_d-1}{2}(\frac{u_{pr}}{a_r})]^{2\gamma_d/(\gamma_d-1)}-\frac{1}{DPR}\} \quad (5)$$

$$x(0)=0 \quad , \quad \dot{x}(0)=0$$

In which d_l is the launch tube, m_{pr} is the projectile mass, x_{pr} is the position of the projectile inside the launch tube, t_{pr} is the time during projectile motion, P_b is the shock pressure at the projectile base and P_{l0} is the initial launch tube pressure. u_{pr} is the projectile speed, a_r and p_r are the sound speed and the pump tube pressure at the burst of second diaphragm. DPR is defined as the ratio p_r / p_{l0}.

3. GAS GUN DESCRIPTION

The gas gun used in this study was developed by the authors of this work at Bu-Ali Sina University. The gun was designed for the pressure of 1000 bar and was equipped with necessary instrumentations such as pressure sensors and velocity measurement.

3. 1. The gun Specifications The general view of the gas gun used in this work is illustrated in Figure 2. The gas gun components are given in Table 1. The lengths of the gas components are shown in Figure 1. The light gas such as air or nitrogen is compressed in the high pressure chamber. Another light gas such as helium is compressed in the pump tube. For testing, the electro-pneumatic valve is opened allowing the high pressure fluid to flow to break the first diaphragm between the chamber and the pump tube. As a result of the first diaphragm rupture, the piston is accelerated in the pump tube and compresses the gas ahead. When the pressure of the gas reaches a certain level, the second diaphragm is burst, the projectile is accelerated in the launch tube and piston is trapped by the conic high pressure tube. The conic tube depicted in Figure 3 can move freely on a rail mounted on a separate chassis. This allows the piston to be taken out from the high pressure conic tube after each test. The geometry of the diaphragm is shown in Figure 4(a). The general view of a diaphragm before and after rupture is also shown in Figure 4(b). The petalling observed in the diaphragm indicates that it has quite symmetrically opened which is an important requirement in the design of gas guns.

This requirement is met if the crossed grooves in the diaphragms are designed properly. The dimensions and the general views of a piston after and before test are presented in Figure 5. The empty space in the back of piston is to seal the piston from the pump tube wall to

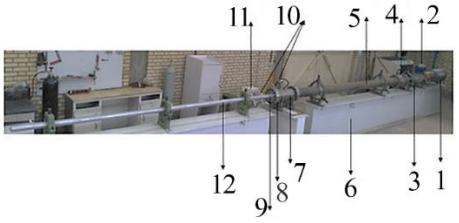

Figure 2. A general view of the gas gun

TABLE 1. The components of the gas gun

	Component		Component
1	High pressure chamber (OD=24, ID=10cm)	7	High pressure conic tube (OD=16cm) (ID_1=4, ID_2=10cm)
2	Electro-pneumatic valve	8	Second diaphragm
3	First diaphragm	9	Projectile initial position
4	Piston initial position	10	Pressure sensors
5	Pump tube (OD=18, ID=10cm)	11	Data logger
6	Chassis	12	Launch tube (OD=7, ID=4cm)

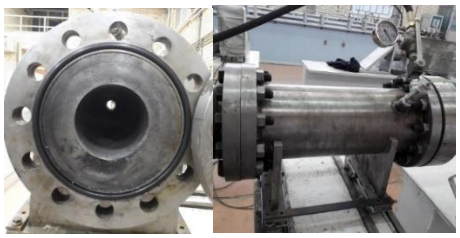

Figure 3. The conic segment of the gas gun

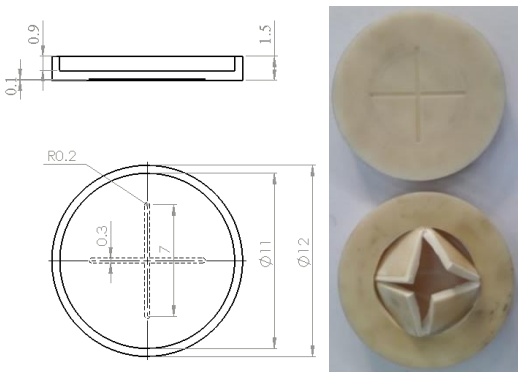

(a) (b)

Figure 4. (a) geometry of diaphragm, (b) view of a diaphragm before and after burst

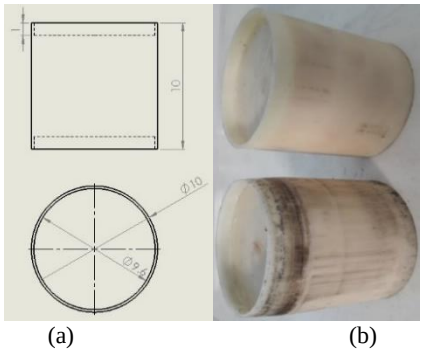

(a) (b)

Figure 5. (a) The geometry of the piston, (b) the general view of a piston before and after test

prevent gas leakage which may result in reducing the piston speed during its motion in the pump tube. A typical projectile before and after impact is shown in Figure 6. The piston, diaphragm and projectile are all made of Teflon.

3. 2. Features of the Gas Gun In order to obtain an initial impression of the gas gun performance, number of tests were carried out for two cases: (i) the pump tube pressure remained constant (10 bars) and the chamber pressure varied from 70 to 250 bars, and (b) the chamber pressure was kept unchanged (150 bars) and the pump tube pressure varied between 0 and 35 bars. Variation of projectile velocity versus the chamber pressure is shown in Figure 7.

As the figure suggests, for a fixed pump tube pressure, the projectile velocity increases with the chamber pressure. However, variation of projectile velocity versus the pump pressure shown in Figure 8 indicates that for a fixed chamber pressure, the projectile velocity converges to a constant level for the pump pressures greater than 35 bars. This important finding means that for a two stages gas gun there is an optimum pressure for pump tube. The effect of projectile mass was also examined using two masses of 400 and 600 g but only a slight difference was observed in the projectile velocity .

Figure 6. The general view of a projectile before and after impact

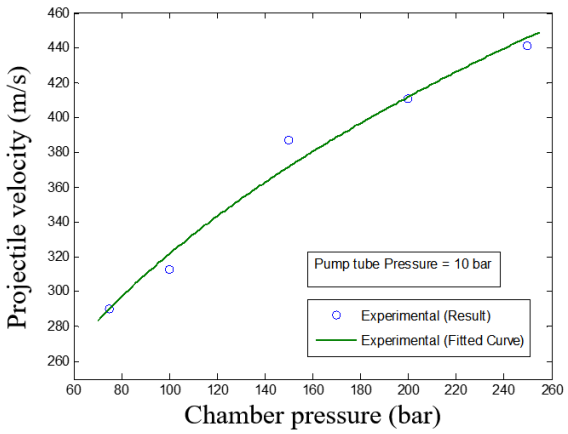

Figure 7. Variation of projectile velocity versus the chamber pressure for a pump tube pressure of 10 bars

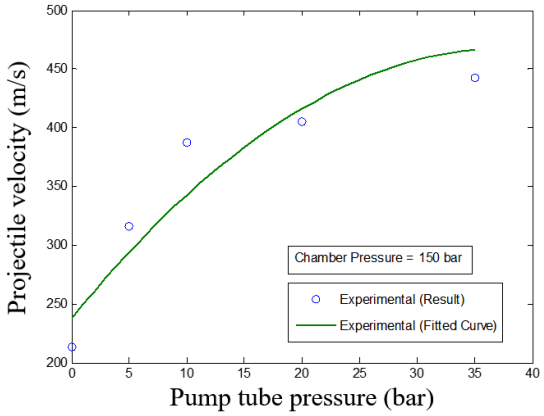

Figure 8. Variation of projectile velocity versus the pump tube pressure for a chamber pressure of 150 bars

The pressure-time histories of the light gas in the high pressure conic and launch tubes were recorded by two Kistler pressure sensors installed in the conic tube right before the second diaphragm and in the launch tube just after the second diaphragm. Typical result for the pump pressure of 10 bars and the chamber pressure of 100 bars is illustrated in Figure 9. The results shown in this figure are highly beneficial as the instant of the burst of the first and the second diaphragms can be detected on the figure. This information is very useful as they can be used to trace the position of the piston inside the pump tube at the time when the second diaphragm is burst. It is highly important to note that the position of piston at the rupture of second diaphragm is a key parameter in design of a gas gun. The reason is that it controls the pressure behind the projectile after the rupture of the second diaphragm. The reason for the oscillations after the first diaphragm's burst is that after the burst shock waves are produced in the chamber. The shock waves begin to travel down to the end of shock tubes and reflect to the piston. These incident and reflected waves hit the piston and change the pressure ahead of the piston resulting in oscillatory pressure after the burst of the first diaphragm.

4. NUMERICAL SIMULATIONS

Numerical simulations were performed using the commercial code Autodyn which is widely used to solve a wide range of high rate and nonlinear problems of fluid and solid mechanics. Autodyn employs Lagrangian, Eulerian, Arbitrary Lagrangian/Eulerian method (ALE) and smoothed particle hydrodynamics method (SPH) solvers to connect the finite element method (FEM) for solving dynamics of structures and Finite volume method (FVM) for solving computational fluid dynamics (CFD).

The main objective of the simulations in this work is (i) to study the effect of gas gun parameters on its performance and (ii) to predict the parameters such as the position and velocity of piston during the test which are either very difficult or impossible to be measured by experiment.

4. 1. Numerical Model Description The numerical model of the gun is depicted in Figure 10. As it is observed in the model, for mesh generation of fluid media such as the tubes, the chamber and the environment, Eulerian element and for the solid components such as piston and projectile, Lagrangian elements have been used. The number of elements have been enough to ensure that convergence has reached in the solution.

The ideal gas model was used for air as the fluid in the gas gun. The thermodynamic properties of the gas are provided in Table 2. As stated before, piston, projectile and diaphragms were made of a polymeric material, Teflon. The elasto-plastic properties of the Teflon are given in Table 3. The boundary conditions in the numerical model are shown in Figure 11. The fixed borders defined between the gas and the solids in pump and launch tubes and moving borders between the gas and piston and projectile were described as the boundary

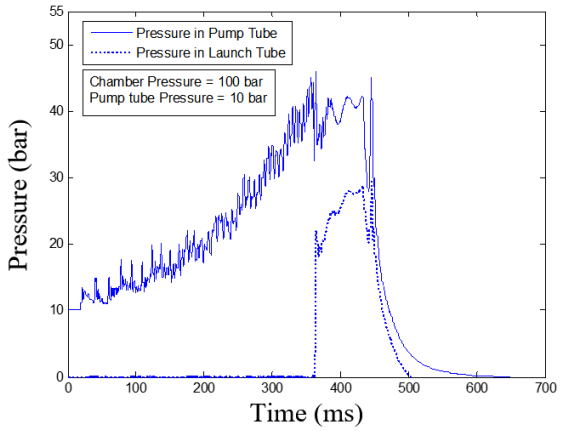

Figure 9. Pressure-time histories for pump tube pressure of 10 bars and the chamber pressure of 100 bars

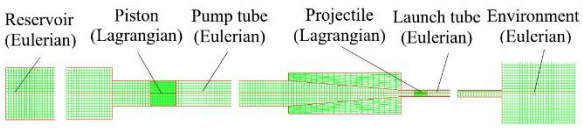

Figure 10. The numerical model of the gun

TABLE 2. The thermodynamic properties of the gas

Density (ρ)	1.225 kg/m^3
Specific heat (C_p)	1.004 kJ/kg.K$^\circ$
Specific heat ratio $\gamma = C_p/C_v$	1.4

TABLE 3. The elaso-plastic properties of Teflon

Density (ρ)	1000 kg/m^3
Elastic modulus (E)	2532 MPa
Yield stress (σ_y)	40 MPa

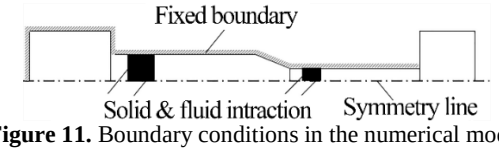

Figure 11. Boundary conditions in the numerical model

conditions. The pump tube and chamber initial pressures have been defined as the initial conditions. The conditions of air inside and out of the launch tube before firing have been described as initial conditions.

4. 2. Numerical Model Validation The numerical model was validated by comparing a number of quantities predicted by numerical simulation and measured from the experiment. A comparison between the numerical and experimental pressure-time histories behind the second diaphragm is shown in Figure 12.

As the figure indicates, a reasonable agreement is observed between the numerical prediction and the experimental measurement. A comparison between the numerical and experimental variation of projectile velocity versus chamber pressure is also illustrated in Figure 13. Although, the numerical predictions are relatively accurate for lower chamber pressure, their difference with the experimental results increases for higher pressures. The reason may be due to the assumption of ideal gas and isentropic flow which may not be accurate enough for higher pressures. The difference for the pressure of 250 bars is, however, less than 10% and quite acceptable.

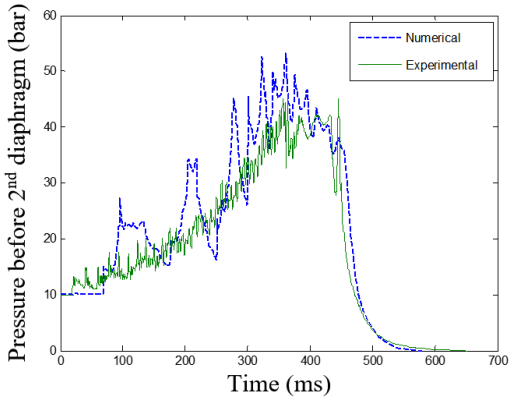

Figure 12. A comparison between the numerical and experimental pressure-time histories behind the second diaphragm

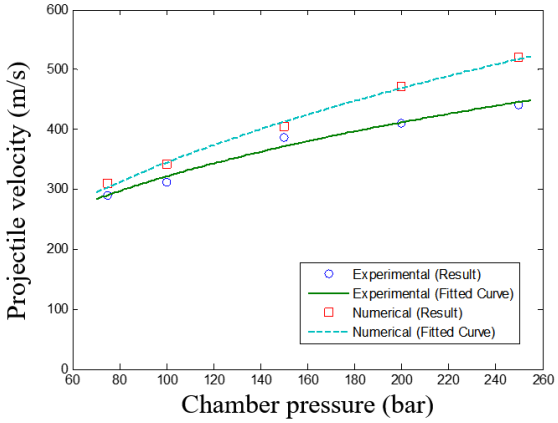

Figure 13. A comparison between the numerical and experimental variation of projectile velocity versus chamber pressure

4. 3. Numerical Results As stated before, the numerical simulations were carried out to predict the quantities which are difficult or costly to be measured by experiment. One of the quantities is the speed of piston in the pump tube. The piston speed-time histories for three chamber pressures are shown in Figure 14. As the figure suggests, piston speed begins to decline after reaching a maximum and stops completely when is trapped by the conic tube. Variation of piston speed versus the chamber pressure is illustrated in Figure 15. As the figure indicates, the piston speed can reach to a speed of 600 m/s for the pressure of 250 bars.

Variation of the projectile speed inside the launch tube is presented in Figure 16. As can be seen, the velocity curves for all projectile masses are nearly flattened at the position x=4 m, i.e. at the muzzle of the launch tube. This means that the length of launch tube is enough to reach the maximum velocity at firing. The position of piston with time in the pump tube for the pump tube pressure of 10 bars and the chamber pressure of 100 bars is demonstrated in Figure 17. This is very

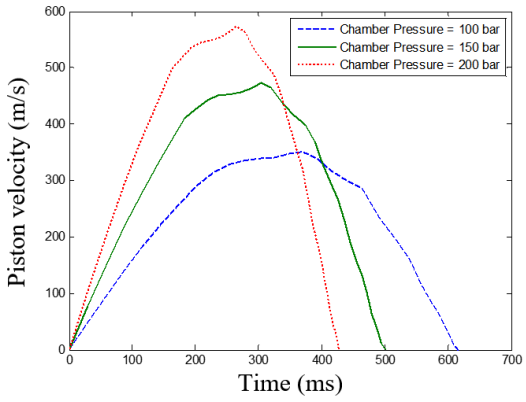

Figure 14. The piston speed-time histories for three chamber pressures

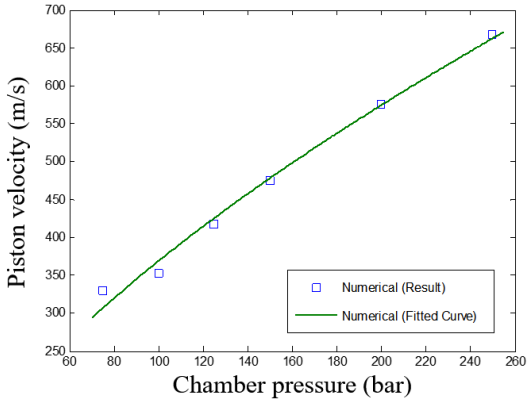

Figure 15. Variation of piston speed versus the chamber pressure

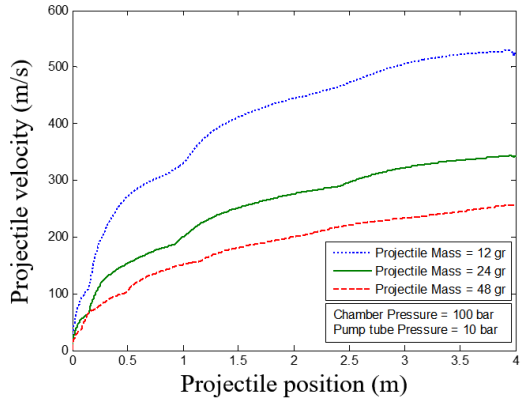

Figure 16. Variation of the projectile speed inside the launch tube

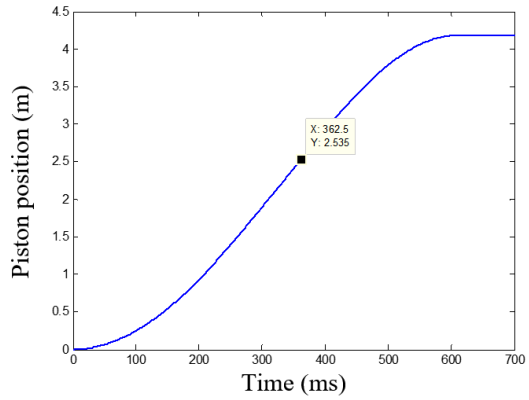

Figure 17. The position of piston with time in the pump tube for the pump tube pressure of 10 bars and the chamber pressure of 100 bars

important graph as it shows the position of the piston inside the pump tube when the second diaphragm is burst. The coordinates of the position (x=362.5 s, y=2.535 m) shown on the graph imply that the second diaphragm is broken at the time 362.5 s and when the piston has travelled a distance of y=2.535 m from the pump tube beginning. The rupture time of the second diaphragm is obtained from a graph typically shown in Figure 9.

5. DISCUSSION

In this section, the effects of various parameters on gas gun performance studied by numerical simulation, Rajesh theory and experiment are compared and various features of the gas gun are explored. Velocity-time histories of piston when moving in pump tube are shown in Figure 18. As it is observed a reasonable agreement is seen between the numerical prediction and the analytical results.

Variation of piston speed versus the chamber pressure is illustrated in Figure 19. Again, the maximum difference between the numerical and analytical results occurs for higher pressures and is around 10% which is acceptable. Variation of projectile speed versus the chamber pressure is depicted in Figure 20. As the figure suggests, the numerical, experimental and theoretical results are relatively close to each other, although Rajesh method and numerical simulations slightly overpredict

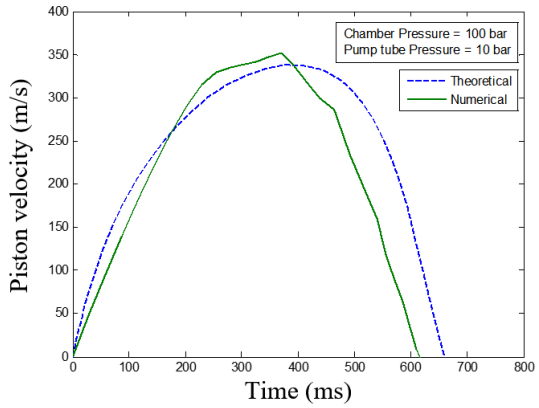

Figure 18. Velocity-time histories of piston

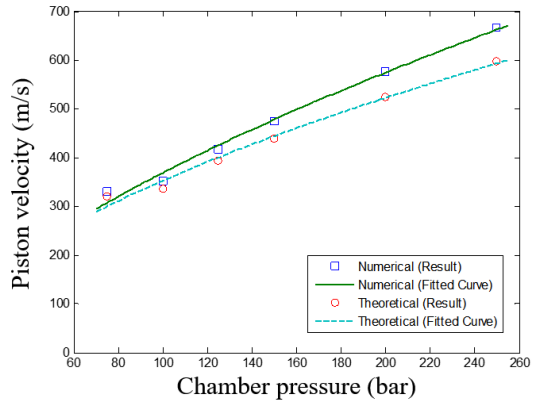

Figure 19. Variation of piston speed versus the chamber pressure

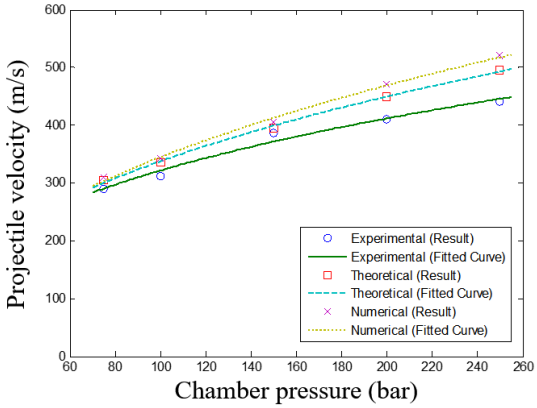

Figure 20. Variation of projectile speed versus the chamber pressure

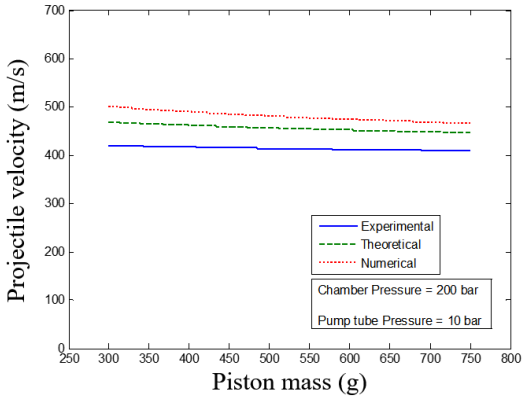

Figure 22. Variation of projectile velocity versus the piston mass

the projectile velocity. However, this overprediction is not as big and varies from zero for low pressures to about 10% for higher pressures.

Variation of projectile velocity versus the projectile mass is presented in Figure 21. As it is seen, the numerical and analytical curves nearly coincide. Also, and as it was stated in section 3, the projectile velocity is not significantly affected by the projectile mass, at least for the range of mass variation in this work (5 to 50 g).

The differences between analytical and experimental results that are seen in Figures 18 to 22 are partly due to some simplifications such as the isentropic and ideal gas assumption for the fluid flow in the tube of the gas gun. Variation of projectile velocity versus the piston mass is demonstrated in Figure 22. The figure reveals that the projectile velocity is also not influenced by the mass of piston, for the range of mass variation in this work (250 to 750 g).

May be the most important issue in the design of a two-stages gas gun is the relation between the gas pressure in pump tube, the chamber's pressure and the projectile velocity. This has been shown in a three-dimensional diagram in Figure 23.

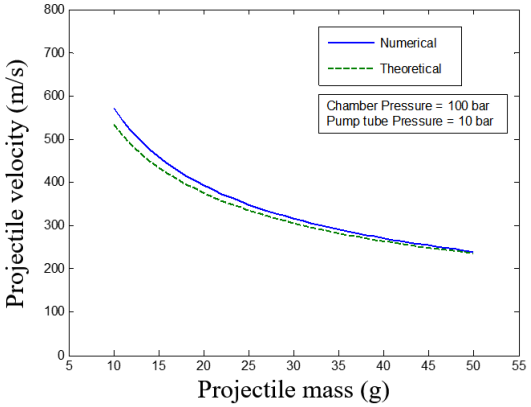

Figure 21. Variation of projectile velocity versus the projectile mass

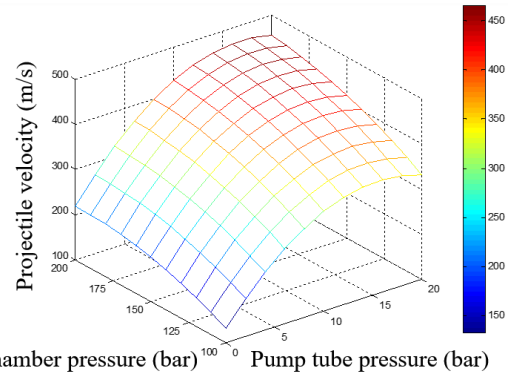

Figure 23. The 3-D working diagram for variation of projectile velocity versus pump and chamber pressures

The surface of the diaphragm can be described by the following equation:

$$V = -133.15 + 25.68P_2 + 3.56P_1 + 0.02P_1P_2 - 0.89P_2^2 - 0.009P_1^2 \quad (4)$$

Having kept P_1 or P_2 fixed and derivating Equation (6) with respect to P_2 or P_1, the maximum velocity of the projectile can be obtained.

7. REFERENCES

1. Majzoobi, G., Kazemi, P. and Pipelzadeh, M., "Determination of the constants of material models using inverse taylor test", ***Experimental Techniques***, Vol. 40, No. 2, (2016), 609-620.
2. Atrian, A., Majzoobi, G., Nourbakhsh, S., Galehdari, S. and Nejad, R.M., "Evaluation of tensile strength of al7075-sic nanocomposite compacted by gas gun using spherical indentation test and neural networks", ***Advanced Powder Technology***, Vol. 27, No. 4, (2016), 1821-1827.
3. Lamberson, L., "Investigations of high performance fiberglass impact using a combustionless two-stage light-gas gun", ***Procedia Engineering***, Vol. 103, (2015), 341-348.

4. Majzoobi, G., Morshedi, H. and Farhadi, K., "The effect of aluminum and titanium sequence on ballistic limit of bi-metal 2/1 fmls", ***Thin-Walled Structures***, Vol. 122, (2018), 1-7.
5. Hardage, B., "Design and construction of a helium gas gun for hypervelocity impact", ***Proceedings of the Oklahoma Academy of Science***, Vol. 45, (1965), 129-138.
6. Combs, S., Foust, C., Gouge, M. and Milora, S., "Acceleration of small, light projectiles (including hydrogen isotopes) to high speeds using a two-stage light gas gun", ***Journal of Vacuum Science & Technology A: Vacuum, Surfaces, and Films***, Vol. 8, No. 3, (1990), 1814-1819.
7. Smith, F., "Theory of a two-stage hypervelocity launcher to give constant driving pressure at the model", ***Journal of Fluid Mechanics***, Vol. 17, No. 1, (1963), 113-125.
8. Bogdanoff, D. and Miller, R.J., "Improving the performance of two-stage gas guns by adding a diaphragm in the pump tube", ***International Journal of Impact Engineering***, Vol. 17, No. 1-3, (1995), 81-92.
9. Bogdanoff, D.W., "Optimization study of the ames 0.5 ″two-stage light gas gun", ***International Journal of Impact Engineering***, Vol. 20, No. 1-5, (1997), 131-142.
10. Doolan, C. and Morgan, R., "A two-stage free-piston driver", ***Shock Waves***, Vol. 9, No. 4, (1999), 239-248.
11. Moritoh, T., Kawai, N., Nakamura, K.G. and Kondo, K.-i., "Optimization of a compact two-stage light-gas gun aiming at a velocity of 9 km/s", ***Review of Scientific Instruments***, Vol. 72, No. 11, (2001), 4270-4272.
12. Lexow, B., Wickert, M., Thoma, K., Schäfer, F., Poelchau, M. and Kenkmann, T., "The extra-large light-gas gun of the fraunhofer emi: Applications for impact cratering research", ***Meteoritics & Planetary Science***, Vol. 48, No. 1, (2013), 3-7.
13. Putzar, R. and Schaefer, F., "Emi's twingun concept for a new light-gas gun type hypervelocity accelerator", ***Procedia Engineering***, Vol. 103, (2015), 421-426.
14. Linhart, J. and Cattani, F., "Theory of a multistage light gas gun", ***Acta Astronautica***, Vol. 61, No. 7-8, (2007), 617-625.
15. Glenn, L.A., "Design limitations on ultra-high velocity projectile launchers", ***International Journal of Impact Engineering***, Vol. 10, No. 1-4, (1990), 185-196.
16. Fredenburg, D.A., Thadhani, N.N. and Vogler, T.J., "Shock consolidation of nanocrystalline 6061-t6 aluminum powders", ***Materials Science and Engineering: A***, Vol. 527, No. 15, (2010), 3349-3357.
17. Francesconi, A., Pavarin, D., Bettella, A. and Angrilli, F., "A special design condition to increase the performance of two-stage light-gas guns", ***International Journal of Impact Engineering***, Vol. 35, No. 12, (2008), 1510-1515.
18. Rajesh, G., Lee, J., Back, S. and Kim, H.D., "A theoretical study for the design of a new ballistic range", ***Journal of mechanical Science and Technology***, Vol. 20, No. 7, (2006), 1019-1029.
19. Rajesh, G., Kim, H., Setoguchi, T. and Raghunathan, S., "Performance analysis and enhancement of the ballistic range", ***Proceedings of the Institution of Mechanical Engineers, Part G: Journal of Aerospace Engineering***, Vol. 221, No. 5, (2007), 649-659.
20. Rajesh, G., Mishra, R., Kang, H. and Kim, H., "Computational analysis of the compressible flow driven by a piston in a ballistic range", ***Journal of Thermal Science***, Vol. 16, No. 4, (2007), 360-369.
21. Doolan, C., *A two-stage light gas gun for the study of high speed impact in propellants*. 2001, Aeronautical And Maritime Research Lab Salisbury (Australia) Weapons Systems Div.
22. Kawai, N., Tsurui, K., Hasegawa, S. and Sato, E., "Single microparticle launching method using two-stage light-gas gun for simulating hypervelocity impacts of micrometeoroids and space debris", ***Review of Scientific Instruments***, Vol. 81, No. 11, (2010), 115105.
23. Schäfer, F. and Janovsky, R., "Impact sensor network for detection of hypervelocity impacts on spacecraft", ***Acta Astronautica***, Vol. 61, No. 10, (2007), 901-911.
24. Jones, A.H., Isbell, W. and Maiden, C., "Measurement of the very-high-pressure properties of materials using a light-gas gun", ***Journal of Applied Physics***, Vol. 37, No. 9, (1966), 3493-3499.

Performance of a Two-stages Gas Gun: Experimental, Analytical and Numerical Analysis

G. H. Majzoobi[a], M. H. Ghaed Rahmati[a], M. Kashfi[b]

[a] *Department of Mechanical Engineering, Bu-Ali Sina University, Hamedan, Iran*
[b] *Department of Mechanical Engineering, Ayatollah Boroujerdi University, Boroujerd, Iran*

P A P E R I N F O

Paper history:
Received 21 July 2018
Received in revised form 03 March 2018
Accepted 19 May 2019

Keywords:
Two Stages Gas Gun
Rajesh Theory
Simulation
Projectile
Autodyn

چکیده

تفنگ‌های گازی دومرحله‌ای جهت مقاصد مختلفی به‌ویژه بررسی رفتار مواد در نرخ کرنش بالا مورداستفاده قرار می‌گیرند. در این پژوهش، عملکرد یک تفنگ گازی دومرحله‌ای توسط روابط تحلیلی بر پایه تحقیقات راجش و شبیه‌سازی عددی بر پایه روش اجزا محدود و استفاده هم‌زمان از المان‌های اویلری و لاگرانژی موردبررسی قرارگرفته است. معادلات حاکم بر حرکت پیستون و پرتابه حل‌شده و اثرات فشار مخزن، فشار لوله پمپ و جرم پیستون بر عملکرد آن موردبررسی قرارگرفته است. نتایج روش‌های عددی و تحلیلی با استفاده از دستگاه طراحی‌شده توسط نویسندگان به‌صورت آزمایشگاهی صحه‌گذاری گردیده است. مقایسه بین نتایج تحلیلی، عددی و تجربی نشان داد که نظریه پیشنهادشده توسط راجش و همچنین، شبیه‌سازی توانسته است عملکرد تفنگ گازی دومرحله‌ای را به خوبی پیش‌بینی کند. همچنین، یک نمودار سه‌بعدی برای پیش‌بینی سرعت پرتابه بر اساس فشارهای مخزن و لوله پمپ ارائه‌شده است.

***doi**: 10.5829/ije.2019.32.05b.18*